11.B4 The influence of horizontal convective rolls on the morphology of low-level rotation in idealized simulations of supercell thunderstorms

CHRISTOPHER J. NOWOTARSKI,* PAUL M. MARKOWSKI, AND YVETTE P. RICHARDSON

Department of Meteorology, The Pennsylvania State University, University Park, PA

GEORGE H. BRYAN

National Center for Atmospheric Research, Boulder, CO

1. Introduction

The origins, evolution, and characteristics of low-level rotation in supercell thunderstorms have attracted significant research attention over the past several decades, because most significant tornadoes are spawned from these storms. In addition to observation and theory, numerical simulations have been utilized to investigate this issue (e.g., Klemp and Wilhelmson 1978; Rotunno and Klemp 1985; Wicker and Wilhelmson 1995). Through idealized numerical simulations, the sensitivity of low-level rotation to environmental parameters such as the wind profile, moisture, and buoyancy has been extensively investigated (e.g., Gilmore and Wicker 1998; Mccaul and Weisman 2001; Parker 2012). The effects of processes such as cyclic mesocyclogenesis (Adlerman et al. 1999) and storm interaction (Bluestein and Weisman 2000) on low-level roatation have also been studied using simulations.

Most idealized simulation studies assume a horizontally homogeneous base state, neglecting the role of friction and surface fluxes of heat and moisture in the evolution of the storm and its environment. Supercell thunderstorms are often found in an environment with near-surface instability generated through daytime solar heating of the surface that results in boundary layer convection. Indeed, this convection is responsible for mixing and deepening of the boundary layer. Whereas some previous studies have examined the effects of heterogeneity in the storm environment on larger scales (Richardson et al. 2007) and across a thermal boundary (Atkins et al. 1999), few studies have examined the effects of such meso-γ-scale heterogeneity on supercell thunderstorms (Crook and Weisman 1998; Knopfmeier et al. 2008). Crook and Weisman (2008) discovered more rapidly developing gust front vortices and a disruption of the organization of the low-level mesocyclone when the low-level storm environment contained disorganized convection. They speculated that the weakening of such convection in the late afternoon hours is responsible for the apparent increase in the likelihood of tornadogenesis in the early evening. It remains unknown if these findings are robust, especially in a more organized boundary layer.

Given the low-level shear that often accompanies supercell thunderstorms, the convective boundary layer (CBL) surrounding such storms may often be organized in horizontal convective rolls (HCRs). HCRs are a series of counter-rotating horizontal vortices with a characteristic wavelength generally 2–4 times greater than the boundary layer height. When thermally-driven, HCRs are aligned with the boundary layer shear vector so as to minimize the detrimental effects of the shear on the convection (Weckwerth et al. 1997). Within the updraft bands of HCRs, vertical velocities can be as strong as 5 m s^{-1} (Etling and Brown 1993), with potential temperature perturbations up to 0.5 K and water vapor mixing ratio perturbations from 1.5–2.5 g kg^{-1} (Weckwerth et al. 1996). Low-level (0-1 km) vector shear magnitude may also vary by as much as 5 m s^{-1} across HCRs (Markowski and Richardson 2007).

Building on the work of Nowotarski et al. (2010, 2011), this study examines the effects of organized CBL turbulence in the form of HCRs on the morphology of low-level rotation in supercell thunderstorms. We hypothesize that periodic variations in environmental characteristics associated with HCRs may alter the location, strength, and duration of low-level vortices and that such alterations may be dependent on the orientation of HCRs relative to storm motion. Section 2 details the methods employed to simulate idealized supercells in an evironment with HCRs that are perpendicular to storm motion. Section 3 presents the results of our simulations, including an analysis of the heterogeneity in wind shear and instability associated with the simulated CBL as well as the effects of HCRs on supercells simulated therein. In section 4 we discuss the implications of these results and avenues of future research.

2. Methods

2.1 Experiment design

The suite of simulations in this study is composed of four simulations (Fig. 1). The first is the BASE simulation, wherein a convective boundary layer is developed using a horizontally homogeneous thermodynamic base state (Fig. 2, green profiles). A quarter circle, clockwise turning hodograph (Weisman and Klemp 1986) is used and shifted relative to the origin to create HCRs perpendicular to storm motion (Fig. 2). Random temperature perturbations ($\pm$0.1 K) are inserted, and the simulation is initialized with radiation corresponding to 1200Z on 15 May in north-central Oklahoma. As the radiation incident on the surface intensifies and surface fluxes destabilize the boundary layer, convective overturning develops, and by 3 hours into

**Corresponding author address*: Christopher Nowotarski, Department of Meteorology, Pennsylvania State University, 503 Walker Building, University Park, PA 16802; *e-mail*: cjn5012@psu.edu.

the simulation (1500Z) HCRs have developed. At this point, a warm bubble with a temperature perturbation of 3 K, a horizontal radius of 10 km, a vertical radius of 1 km, centered 1 km above the lower surface is inserted into the simulation restart files (the average base state at this time is shown in Fig. 2 in red). In one simulation, CBL EVOLVE, radiative forcing is allowed to continue evolving with time, whereas in CBL FIXED radiation is fixed to the values at the time of the warm bubble initialization. This is done so that in CBL FIXED the storm effects on radiation (i.e., cloud shading) will not influence the evolution of the CBL. The control simulation is intialized using the horizontally averaged sounding from the BASE simulation one hour later than in the CBL FIXED or CBL EVOLVE simulations (Fig. 2, black) because surface fluxes and radiation are turned off in this simulation. Other configurations were tested for the control, but it was found that this set up resulted in values of CAPE, CIN, precipitable water, and a hodograph that were most similar to the simulations with radiation and surface fluxes over the period of the simulation with a mature supercell. All three supercell simulations were run for two hours.

2.2 Model configuration

All simulations are run using CM1, Release 15 (Bryan and Fritsch 2002). CM1 is a moist non-hydrostatic model that solves the compressible governing equations using a split time step, with terms associated with acoustic waves solved on a time step that is 1/6 of the large time step for non-acoustic terms (Klemp and Wilhelmson 1978). In all simulations fifth-order advection with implicit diffusion is used. Subgrid-scale turbulence is modeled using a simplified 1.5-order turbulence kinetic energy (TKE) scheme (Deardorff 1980). Cloud microphysics and precipitation are modeled using the bulk ice phase microphysical parameterization developed by Lin et al. (1983). The Coriolis force is ignored in these simulations. These simulations include parameterizations for long and shortwave radiation (Chou and Suarez 1999), a slab soil model, surface drag, as well as surface heat and moisture fluxes. The domain is 250×200 km with 200-m horizontal grid spacing (sensitivity of HCRs to gridspacing is discussed in section 3) and a stretched vertical grid with 50-m spacing below 3 km and 500-m spacing above 8.5 km. The upper boundary condition is a rigid lid at 18 km with a Rayleigh damping sponge layer above 14 km. Periodic boundary conditions are applied at all lateral boundaries.

3. Results

3.1 CBL characteristics

The characteristics of the simulated HCRs are dependent on the grid spacing used. Theory and observation suggest (Etling and Brown 1993) that roll aspect ratio (wavelength / CBL depth) should be approximately 2-4. Figure 3 shows a time series of roll aspect ratio for three different horizontal grid spacings at times when HCRs are identifiable.[1] Roll onset is earlier in simulations with smaller horizontal grid spacing, and roll aspect ratio tends to increase with horizontal grid spacing. Using the 100-m grid spacing simulation as a benchmark, it is apparent that the 200-m simulation results in rolls with a more realistic aspect ratio than the 500-m grid spacing simulations used in previous work (Nowotarski et al. 2011). Furthermore, the aspect ratio of both the 200-m and 100-m grid spacing simulations are similar and in the expected range, suggesting convergence of HCR characteristics at these grid spacings. As such, we believe our use of 200-m horizontal grid spacing is justified in that it results in physically realistic HCRs.

The heterogeneity associated with the simulated HCRs with 200-m horizontal grid spacing is apparent in Fig. 4 and similar to HCR characteristics found in other studies. Maximum vertical velocity perturbations in the boundary layer of up to 1.5 m s^{-1} are found in roll updraft branches. HCR downdrafts tend to be weaker and wider than areas of updraft. Surface temperature and dewpoint temperature increase by as much as 0.5 K in updraft branches, resulting in as high as a 10% increase in CAPE relative to downdraft branches. Low-level wind shear varies by as much as 3 m s^{-1} across the HCRs.

HCRs also create periodic maxima and minima in vertical vorticity at at the lowest grid level (Fig. 5). Downdraft branches advect higher momentum air from the top of the boundary layer to the surface, resulting in stronger surface winds juxtaposed with weaker winds in updraft branches. This horizontal gradient in wind leads to alternating bands of positive and negative vertical vorticity on the order of 0.001 s^{-1}.

3.2 Comparison of simulated supercells

The warm bubble perturbation triggers deep convection in each simulation that evolves into splitting supercell thunderstorms with a dominant right-mover. Maximum values of vertical velocity (not shown) and vertical vorticity (Fig. 6) are similar in all three simulations. At midlevels (not shown) the storms in all three simulations display similar characteristics associated with midlevel mesocyclones of similar strength and organization.

Low-level horizontal cross sections (Fig. 7) near 90 minutes into each simulation (a time when each storm has a relative maximum in low-level vertical vorticity) show significant differences in the structure and organization of low-level vorticity maxima. The control simulation (Fig. 7a) has a concentrated region of strong vorticity associated with a persistent low-level mesocyclone. Though vorticity maxima of similar magnitude are found in the CBL FIXED supercell (Fig. 7b), these features are more transient and a sustained low-level mesocyclone does not develop in this simulation. Furthermore, the inflow environment of the CBL FIXED storm is riddled with areas of both positive and negative vertical vorticity that are intensified as they approach the storm (presumably through convergence along the gust front and stretching by the storm's updraft). The CBL EVOLVE simulation (Fig. 7c) also has areas of vertical vorticity in its inflow, but these are fewer and generally weaker. This is likely due to weakening of the boundary layer convection owing to cloud shading of the storm inflow evident in the vertical velocity field. The CBL EVOLVE storm develops a low-level mesocyclone similar to the control simulation, perhaps as a result of this weakening in the HCRs.

The development of misocyclone-like vorticity maxima

[1] Rolls become disorganized as the boundary layer deepens because of an increased buoyancy flux and deteriorating low-level shear (shear is mixed out by HCRs in the boundary layer).

along the gust front is also affected by the presence of HCRs. In the CBL FIXED simulation, periodic misovorticies develop along the rear-flank gust front early in the storm's evolution as HCR perturbations intersect the outflow boundary. Such vortices do not develop until later in the control storm, until heterogeneities within the storm outflow (e.g., gust front surges) develop. When they do develop, there are fewer, more widely spaced misovortices along the control rear-flank gust front.

4. Conclusions and future work

The results presented here suggest that HCRs can lead to considerable horizontal heterogeneity in the supercell environment and can influence the morphology of low-level rotation in simulated supercell thunderstorms. Theories of the creation of low-level rotation in supercells generally assume that storm environments are free from pre-existing vertical vorticity; however, this study suggests that HCRs may be a source of pre-existing vertical vorticity (both positive and negative) near the ground. Though not significantly affecting bulk measures of storm strength, HCRs have been shown to have a disruptive effect on the organization of low-level mesocyclones.

Future work, including circulation and trajectory analysis, is aimed at understanding if and how pre-existing vertical vorticity (or other perturbations associated with HCRs) may lead to this apparent disruption. The sensitivity of these results to the orientation of HCRs relative to storm motion is currently being investigated with simulations of parallel HCRs. The results of Crook and Weisman (1998) regarding storm structure and vertical vorticity are largely confirmed by this research. However, our CBL EVOLVE simulation, wherein HCRs were weaker in the near-storm environment owing to anvil shading, suggests that the boundary layer has less effect on low-level supercell properties when the surface heat flux is reduced. This finding may support their hypothesis regarding the effects of the evening decrease in boundary level turbulence on low-level rotation. HCRs also appear to modulate the formation and evolution of misocyclones along the rear-flank gust front. To further understand this process, the authors plan to conduct a series of idealized simulations wherein a simple density current is released into an environment with HCRs, thereby eliminating the effects of heteorogeneities within the storm outflow.

Acknowledgments. This work is supported by NSF grants AGS-0644533 and AGS-1157646. Computing facilities and support were provided by NCAR CISL. The authors also wish to thank Tammy Weckwerth, Jim Marquis, and Nels Shirer for helpful discussions.

REFERENCES

Adlerman, E. J., K. K. Droegemeier, and R. Davies-Jones, 1999: A numerical simulation of cyclic mesocyclogenesis *J. Atmos. Sci.*, **56**, 2045–2067.

Atkins, N. T., M. L. Weisman, and L. J. Wicker, 1999: The influence of preexisting boundaries on supercell evolution. *Mon. Wea. Rev.*, **127**, 2910–2927.

Bluestein, H. B., and M. L. Weisman, 2000: The interaction of numerically simulated supercells initiated along lines. *Mon. Wea. Rev.*, **128**, 3128–3149.

Bryan, G. H., and J. M. Fritcsh, 2002: A benchmark simulation for moist nonhydrostatic numerical models. *Mon. Wea. Rev.*, **130**, 2917–2928.

Chou, M. D., and M. J. Suarez, 1999: A solar radiation parameterization for atmospheric studies. *NASA Tech. Rep.*, **15**, 38 pp.

Crook, N. A., and M. L. Weisman, 1998: Comparison of supercell behavior in a convective boundary layer with that in a horizontally-homogeneous environment, Preprints, *19th Conf. on Severe Local Storms*, Minneapolis, MN, Amer. Meteor. Soc.

Deardorff, J. W., 1980: Stratocumulus-capped mixed layers derived from a three-dimensional model *Bound. Layer Meteor.*, **18**, 495–527.

Etling, D., and R. A. Brown, 1993: Roll vortices in the planetary boundary layer: A review. *Bound. Layer Meteor.*, **65**, 215–248.

Gilmore, M. S., and L. J. Wicker, 1998: The influence of midtropospheric dryness on supercell morphology and evolution. *Mon. Wea. Rev.*, **126**, 943–958.

Klemp, J. B., and R. B. Wilhelmson, 1978: The simulation of three-dimensional convective storm dynamics. *J. Atmos. Sci.*, **35**, 1070–1096.

Knopfmeier, K. H., P. M. Markowski, and Y. P. Richardson, 2008: Numerical simulations of supercells in convective boundary layers, Preprints, *24th Conf. on Severe Local Storms*, Savannah, GA, Amer. Meteor. Soc.

Lin, Y.L., R. D. Farley, and H. D. Orville, 1983: Bulk parameterization of the snow field in a cloud model. *J. Climate Appl. Meteor.*, **22**, 1065–1092.

McCaul, E. W., and M. L. Weisman, 2001: The sensitivity of simulated supercell structure and intensity to variations in the shapes of environmental buoyancy and shear profiles. *Mon. Wea. Rev.*, **129**, 664–687.

Markowski, P. M, and Y. P. Richardson, 2007: Observations of vertical wind shear heterogeneity in convective boundary layers. *Mon. Wea. Rev.*, **135**, 843–861.

Nowotarski, C. J., P. M. Markowski, Y. P. Richardson, and G. H. Bryan, 2010: Simulating supercell thunderstorms in a horizontally heterogeneous convective boundary layer, Preprints, *25th Conf. on Severe Local Storms*, Denver, CO, Amer. Meteor. Soc.

———, ———, ———, and ———, 2011: Interactions between simulated supercell thunderstorms and dry boundary layer convection, Preprints, *14th Conf. on Mesoscale Processes*, Los Angeles, CA, Amer. Meteor. Soc.

Parker, M.D., 2012: Impacts of lapse rates on low-level rotation in idealized storms. *J. Atmos. Sci.*, **69**, 538–559.

Richardson, Y. P., K. K. Droegemeier, and R. P. Davies-Jones, 2007: The influence of horizontal environmental variability on numerically simulated convective storms, Part I: Variations in Vertical Shear. *Mon. Wea. Rev.*, **135**, 3429–3455.

Rotunno, R., and J.B. Klemp, 1985: On the rotation and propagation of simulated supercell thunderstorms. *J. Atmos. Sci.*, **42**, 271–292.

Weckwerth, T. M., J. W. Wilson, and R. M. Wakimoto, 1996: Thermodynamic variability within the convective boundary layer due to horizontal convective rolls. *Mon. Wea. Rev.*, **124**, 769–784.

———, ———, ———, and N. A. Crook, 1997: Horizontal convective rolls: Determining the environmental conditions supporting their existence and characteristics. *Mon. Wea. Rev.*, **125**, 505–526.

Weisman, M. L., and J. B. Klemp, 1986: Characteristics of isolated convective storms. *Mesoscale Meteorology and Forecasting*, P. Ray, Ed., Amer. Meteor. Soc., 331–358.

Wicker, L. J., and R. B. Wilhelmson, 1995: Simulation and analysis of tornado development and decay within a three-dimensional supercell thunderstorm. *J. Atmos. Sci.*, **52**, 2675–2703.

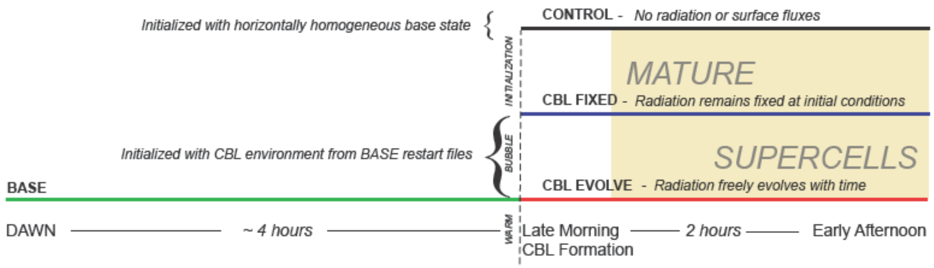

FIG. 1: Schematic diagram illustrating the design of each simulation.

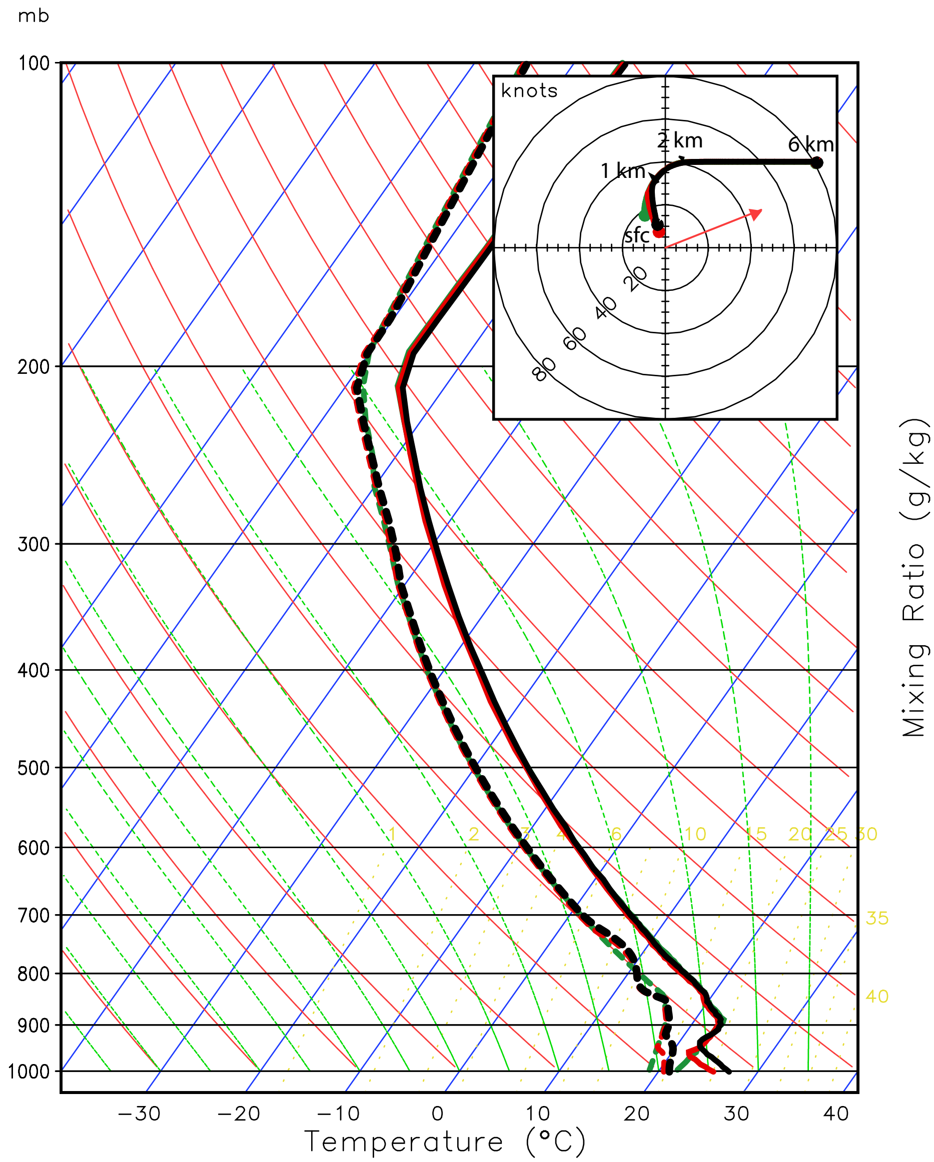

FIG. 2. Skew-T log-P diagram and hodograph of base states used for simulations. Solid profiles are temperature and dashed profiles are dewpoint temperature. The green sounding is used to initialize the BASE simulation. After a CBL has formed, the horizontally averaged sounding (red) is used to intialize the CBL FIXED and CBL EVOLVE simulations. The black sounding is the horizontal average of the BASE simulation at a time corresponding to the midpoint of the CBL FIXED and CBL EVOLVE simulation and is used to intialize the control simulation. The red arrow on the hodograph indicates average storm motion.

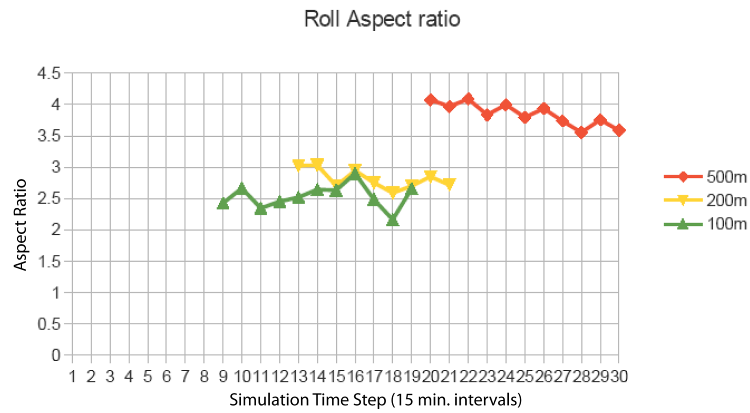

FIG. 3. Time series of roll aspect ratio for three different horizontal grid spacings. Time is expressed in simulation timestep intervals of 5 minutes.

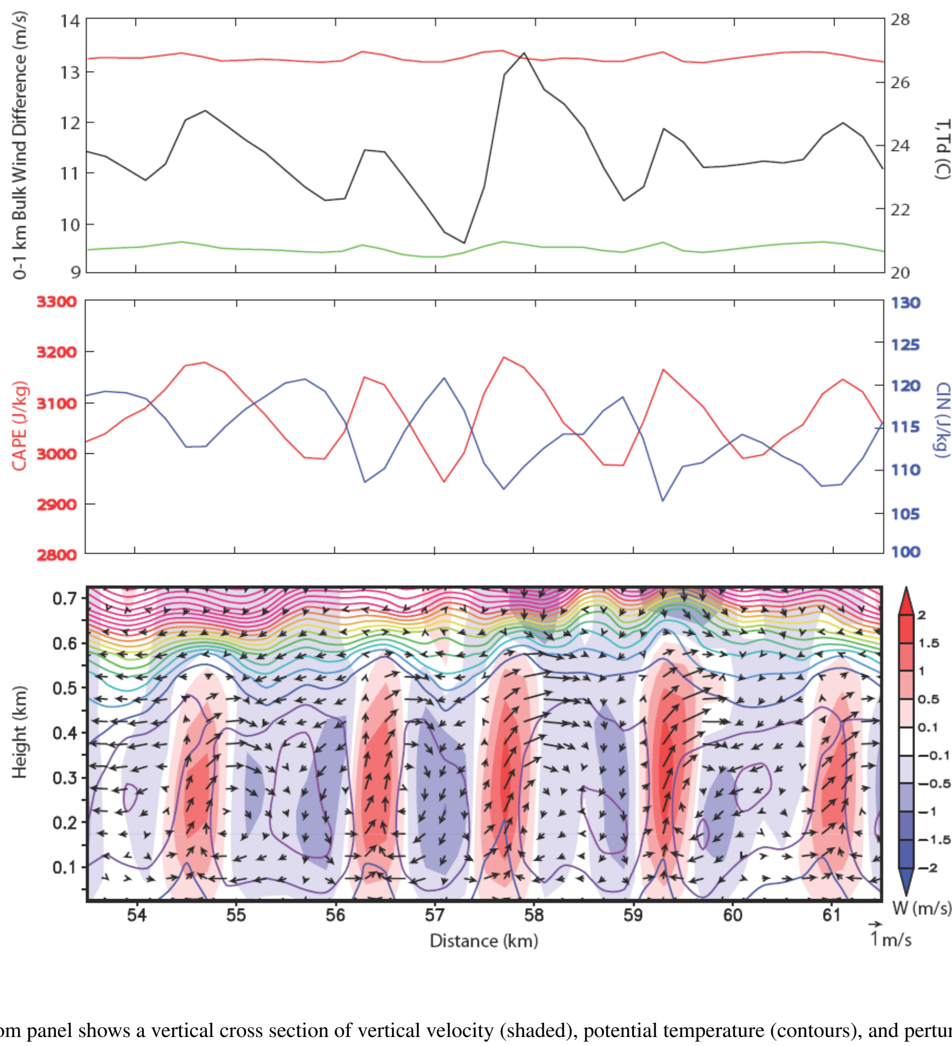

FIG. 4. The bottom panel shows a vertical cross section of vertical velocity (shaded), potential temperature (contours), and perturbation velocity in the plane of the cross section. The middle panel shows CAPE (red) and CIN (blue) corresponding to the location in the cross section below. The top panel shows 0-1 km bulk wind difference (black), temperature (red), and dewpoint temperature (green) at the lowest grid level (25 m) corresponding to the location in the cross section below.

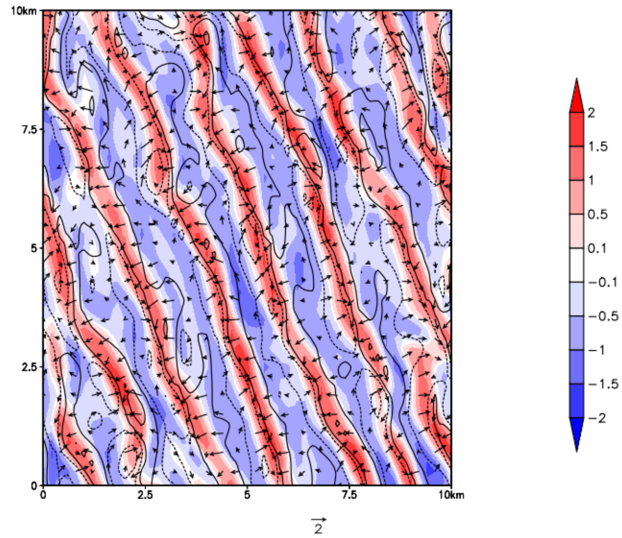

FIG. 5. Horizontal cross section of BASE simulation showing vertical velocity (shaded) at 250 m AGL, perturbation wind vectors at 25 m AGL, and vertical vorticity (countours, 0.001 s^{-1} solid, -0.001 s^{-1} dashed) at 25 m AGL.

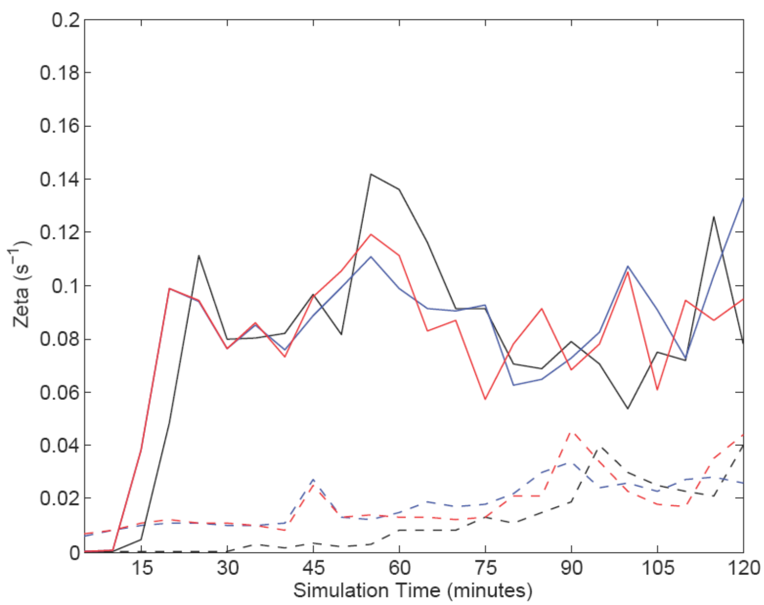

FIG. 6. Time series of maximum vertical vorticity 4 km AGL (solid lines) and at the lowest grid level (dashed lines) associated with the right-moving supercell in the control (black), CBL FIXED (blue), and CBL EVOLVE (red) simulations.

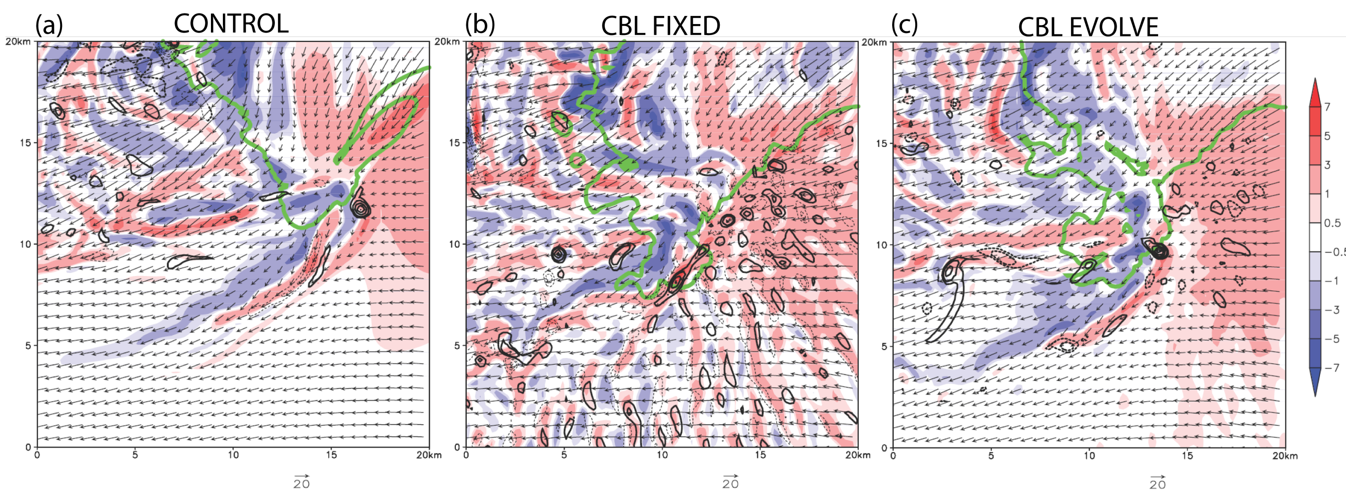

FIG. 7. Horizontal cross-sections of vertical velocity at 275 m AGL (shaded), vertical vorticity at 25 m AGL (black; -0.02, -0.01, -0.005 s^{-1} dashed contours; 0.005, 0.01, 0.02, 0.03, 0.04 s^{-1} solid contours), and storm relative winds at 25 m AGL for the (a) control (b) CBL FIXED and (c) CBL EVOLVE supercells. Rainwater mixing ratio > 0.1 g kg^{-1} is outlined in green.